Histochemistry (1987) 87:339–349

Histochemistry

Ultrastructural distribution of Ca^{++} within neurons

An oxalate pyroantimonate study

M. Mata*, J. Staple, and D.J. Fink
Neurology Research Laboratory, University of Michigan, and
Veterans Administration Medical Center, 2215 Fuller Road, Ann Arbor, MI 48105, USA

Accepted May 8, 1987

Summary. We used the oxalate-pyroantimonate technique to determine the ultrastructural distribution of Ca^{++} in neurons of the rat sciatic nerve. The content of the precipitate was confirmed by X-ray microanalysis and appropriate controls. In the cell bodies of the dorsal root ganglia, Ca^{++} precipitate was found in the Golgi, mitochondria, multivesicular bodies and large vesicles of the cytoplasm but not in lysosomes, and was prominently absent from regions of rough endoplasmic reticulum and ribosomes. It was seen in the nucleus but not in the nuclear bodies or nucleolus.

Within the axon itself, Ca^{++} precipitate was also found sequestered in mitochondria and smooth endoplasmic reticulum. In addition Ca^{++} precipitate found diffusely throughout the axoplasm exhibited a discrete and heterogeneous distribution. In myelinated fibers the amount of precipitate decreased predictably in the axoplasm beneath the Schmidt-Lanterman clefts and in the paranodal regions at the nodes of Ranvier. This correlated with the presence of dense precipitate in the Schmidt-Lanterman clefts themselves and in the paranodal loops of myelin.

Intracytoplasmic ionic Ca^{++} is maintained at 10^{-7} M by balanced processes of influx, sequestration and extrusion. The irregular distribution of Ca^{++} precipitate in the axoplasm of myelinated fibers suggests that there may be specific regions of preferential efflux across the axolemma.

Introduction

Ca^{++} plays a role in regulating a variety of cell functions. The overall intracellular concentration of free calcium, estimated to be about 10^{-7} M in a number of different cell types (Campbell 1983) is maintained by balanced processes of influx and extrusion of calcium, and sequestration of Ca^{++} in organelles such as the sarcoplasmic reticulum in muscle (Endo 1977) and the mitochondria and endoplasmic reticulum in other cells (Blaustein et al. 1978; Carafoli and Crompton 1976). Rapid shifts in Ca^{++} concentration in a specific region of the cell is responsible for the actin-myosin interaction in muscle contraction (Ebashi and Endo 1968) and the release of vesicles by endocrine cells (Rubin 1970).

In the neuron, Ca^{++} has been implicated as playing a critical role both in normal nerve function and in pathologic states. In normal nerve, intracellular Ca^{++} controls the assembly of tubulin dimers into axonal microtubules (Schliwa 1976), influx of Ca^{++} at the nerve terminal triggers synaptic release of neurotransmitters (Rubin 1970), and intraaxonal Ca^{++} appears critical to the normal mechanism of anterograde axonal transport (Ochs et al. 1977). Following an injury to the axon, the axon beyond the crush undergoes Wallerian degeneration in which a calcium-activated protease destroys normal neurofilaments (Schlaepfer et al. 1985).

We were interested in studying the role of Ca^{++} in the neuronal response to injury, and as a first step used a modification of the oxalate-pyroantimonate technique described by Borgers et al. (1977) to visualize the specific subcellular compartmentalization of Ca^{++} within the peripheral nerve cell. In this method, intracellular Ca^{++} is chelated with oxalate during the primary fixation, other cations are washed out, and the sample then treated with osmium pyroantimonate to create Ca^{++} pyroantimonate precipitates. The "pyroantimonate technique" is not a single procedure but rather a series of methods in which the choice of reaction conditions determines the specificity of the reaction for Ca^{++} (Wick and Hepler 1982). In the variation of the method which we have used, we have demonstrated that the precipitate represents Ca^{++} pyroantimonate by X-ray microanalysis, and by the fact that the precipitate was not present when we deleted the pyroantimonate or treated the ultrathin section with EGTA.

Using other variations of the oxalate technique, other investigators have described the localization of precipitates in the membranes of mitochondria and smooth endoplasmic reticulum within the axon (Duce and Keen 1978; Theron et al. 1975), and within those organelles as well as synaptic vesicles in the carp optic tectum using both the oxalate method and the osmium/bichromate method (Probst 1986). We have confirmed that previously described localization within organelles, but in addition, have studied the distribution of Ca^{++} precipitate within the axoplasm. We have found that the precipitate appears to be localized specifically within reproducible domains in the axon. In this paper, we describe that distribution of Ca^{++} from the nerve cell body to the neuromuscular junction.

Materials and methods

Male Sprague-Dawley rats, 250–300 g, were used in all experiments. The animals were perfused through the heart with 90 mM potassium oxalate in 1.9% sucrose adjusted to pH 7.4 with KOH,

* To whom offprint requests should be sent

at 37° C for 2 min, followed by 3% glutaraldehyde, 0.5% paraformaldehyde, 90 m*M* potassium oxalate, 1.9% sucrose adjusted to pH 7.4 with KOH for approximately 1 h at a constant perfusion rate. At the conclusion of the perfusion, the sciatic nerve, the L4, L5 and L6 dorsal root ganglia, with the corresponding dorsal and ventral roots and the gastrocnemius muscle were removed and maintained in the same fixative solution at 4° C for 2 h. They were then rinsed in 90 m*M* potassium oxalate in 1.9% sucrose, pH 7.4, post-fixed in 1% osmium tetroxide and 2% potassium pyroantimonate for 2 h at room temperature. Unreacted potassium pyroantimonate was washed out by rinsing the tissue in water adjusted to pH 10 with KOH for 15 min. Subsequently, the samples were dehydrated in alcohol and embedded in a Polybed Araldite mixture. Semithin and ultrathin sections were prepared on an LKB Nova ultratome, picked up on uncoated nickel grids and examined without post-staining in a JEOL-100S electron microscope. Occasionally, specimens were stained with uranyl acetate or lead citrate to enhance contrast. All such stained specimens are noted in the figure legends. The nerves from five animals were analyzed.

In order to demonstrate the specificity of the reaction, several controls were performed. In the first control of 2% potassium pyroantimonate was deleted from the post-fixation and 90 m*M* potassium oxalate used in its place. In the second control, the ultrathin sections supported on the grids were washed in 10 m*M* EGTA pH 8 at 60° C for 1 h, with parallel grids washed in water, adjusted to pH 8 with KOH at 60° C for 1 h serving as internal controls. The remainder of the processing steps were unchanged.

X-ray microanalysis was performed on 100–200 nm unstained sections on nickel grids with a JEOL-100CX electron microscope equipped with a KEVEX 3212 SMS-V energy dispersive spectrometer with an accelerating voltage of 100–200 kV, tilt angle of the preparation 35°, and collection time of spectral lines 180–2000 s. The area analyzed ranged from 0.2×0.25 to 0.45×0.60 min.The K_α and K_β Ca^{++} peaks and the L_α and L_β antimonate peaks occur in the same energy region respectively, and their peaks overlap. To demonstrate the presence of Ca^{++}, the spectrums obtained were deconvoluted using the "multiple least squares fit" method developed by Schamber et al. (1977) as adapted to a Nuclear Data 6620 computer.

In other experiments the animals were perfused directly with 3% glutaraldehyde, 0.5% paraformaldehyde, 90 m*M* potassium oxalate in sucrose, omitting the pre-perfusion with 90 m*M* potassium oxalate. The distribution and characteristics of the precipitate were identical to those found after pre-perfusion, but there was better clearance of blood from the capillaries with pre-perfusion. Therefore all the results illustrated here are from animals which had been pre-perfused.

Results

Identification of Ca^{++} in the electron dense precipitate

A fine diffuse precipitate was seen throughout the axoplasm of myelinated and unmyelinated fibers, and in the cytoplasm of dorsal root ganglion cells and Schwann cells. An example of the precipitate in a myelinated axon is shown in Fig. 1A. In order to determine that the precipitate represents calcium pyroantimonate, X-ray microanalysis was performed on selected areas of axoplasm. The energy spectrum obtained from axoplasm containing precipitate is shown in Fig. 1C. The amount of Ca^{++} in the spectrum obtained ranged from 278–403 counts corresponding to 14%–19% of the total counts in the K_α and K_β regions for calcium. The number of counts in the Ca^{++} peak met the standard criterion for significance (Roomans 1980).

When consecutive serial sections were exposed to 10 m*M* EGTA pH 8 at 60° C for 1 h, the precipitate was removed entirely (Fig. 1B) and X-ray microanalysis of the EGTA treated specimens showed that the combined calcium antimonate peak was no longer present (Fig. 1D). Exposing similar sections to ultrapure water adjusted to pH 8 with KOH at 60° C for 1 h had no effect on the precipitate. Furthermore, when potassium pyroantimonate was deleted from the osmium post fixation (substituting 90 m*M* potassium oxalate) no precipitate was found. These controls confirm that the precipitate is a calcium pyroantimonate precipitate.

Results identical to those shown for nerve were obtained in controls using dorsal root ganglion and muscle.

Distribution of Ca^{++} precipitate in the axon

Ca^{++} pyroantimonate precipitate was seen diffusely throughout the axoplasm in both myelinated (Figs. 1A, 2 and 3) and in unmyelinated fibers (data not shown). The precipitate appeared to have a linear longitudinal organization, occurring more commonly in regions of axoplasmic matrix and neurofilaments, but less apparent in the region around microtubules. Fine reticular precipitate was very often seen within the tubulovesicular figures of the smooth endoplasmic reticulum and also in mitochondria (Figs. 1A, 2 and 3). In contrast to previous descriptions using other methods, the precipitate appeared unattached to the organelle membrane. The total amount of precipitate varied somewhate from fiber to fiber, but the distribution within fibers was similar regardless of precipitate density.

In unmyelinated fibers, the distribution of Ca^{++} appeared homogenous along the length of the axon. However, in myelinated fibers, the amount of precipitate varied predictably along the length of the axon. The amount of Ca^{++} precipitate was less in the axoplasm beneath the Schmidt-Lanterman clefts and greater in the axoplasm between clefts (Fig. 2A). This decrease was seen in 89 of the 120 clefts photographed and was found in the ventral roots, the dorsal roots, and in the distal nerve branches within the gastrocnemius muscle, as well as within the body of the axon.

A gradient was also seen around the nodes of Ranvier. The amount of precipitate was usually decreased in the axoplasm under the paranodal loops of myelin, while in the node itself the amount of precipitate was sharply in-

Fig. 1. A Ca^{++} pyroantimonate in the axoplasm of a myelinated fiber. Precipitate is also seen in the smooth endoplasmic reticulum (*arrowhead*) and mitochondria (*arrow*). ×20520, stained with uranyl acetate. *Bar* = 1 μm. **B** Immediate serial section of the same fiber treated with 10 m*M* EGTA pH 8 for 1 h. Note the absence of precipitate. ×20520, stained with uranyl acetate. *Bar* = 1 μm. **C** X-ray microanalysis of axoplasmic precipitate. The overlapping spectrum of the K_α and the K_β peaks of calcium and the L_α and L_β peaks of antimonate obtained are shown. The K_α of calcium occurs at 3.69 KeV. The total counts of calcium in the peak was 403, determined by deconvolution as described in the text. The peaks of osmium (1.91 KeV) and chloride (2.26 KeV) are also seen. (Collection time 2000 s, area 0.25×0.35 μm). **D** X-ray microanalysis of the axoplasm of a myelinated fiber treated with EGTA. The absence of the calcium antimonate peaks correlate with the absence of precipitate as seen in photomicrograph **B**. (Collection time and area as in **C**.)

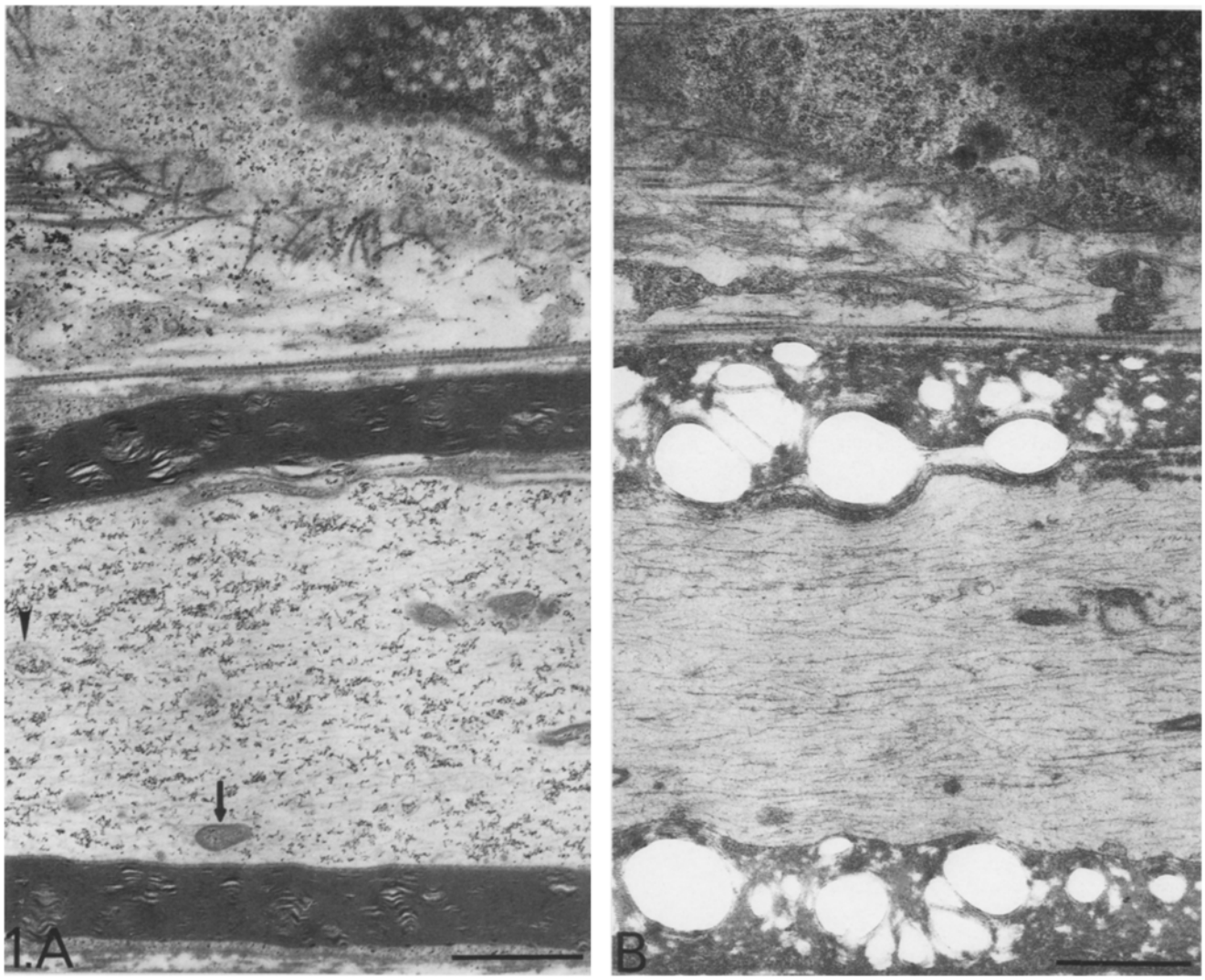
1.A
B

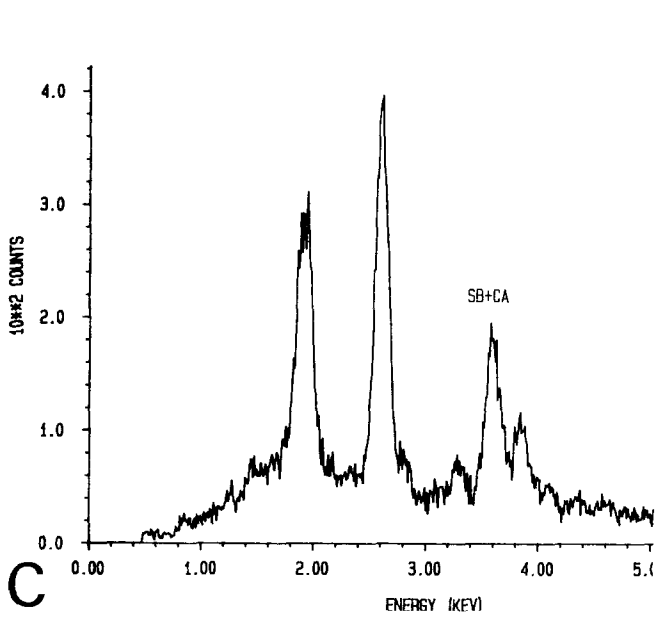
4.0
3.0
2.0
1.0
0.0
10**2 COUNTS
SB+CA
0.00
1.00
2.00
3.00
4.00
ENERGY (KEV)
C

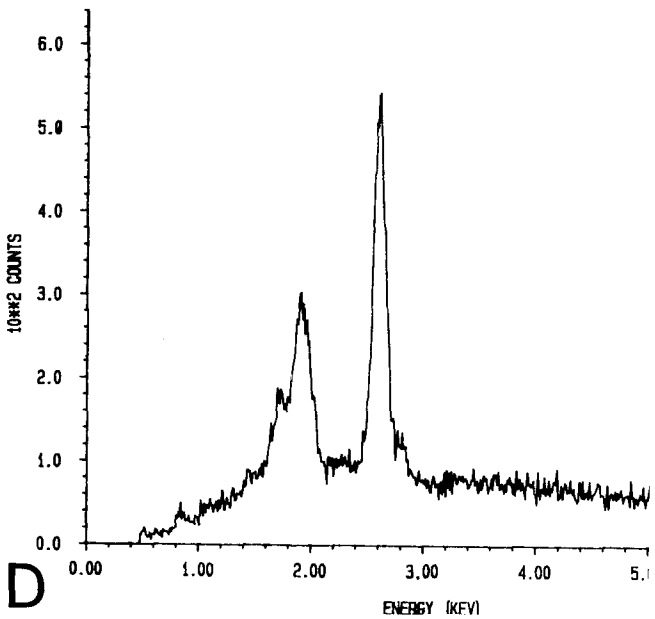
6.0
5.0
4.0
3.0
2.0
1.0
0.0
10**2 COUNTS
0.00
1.00
2.00
3.00
4.00
ENERGY (KEV)
D

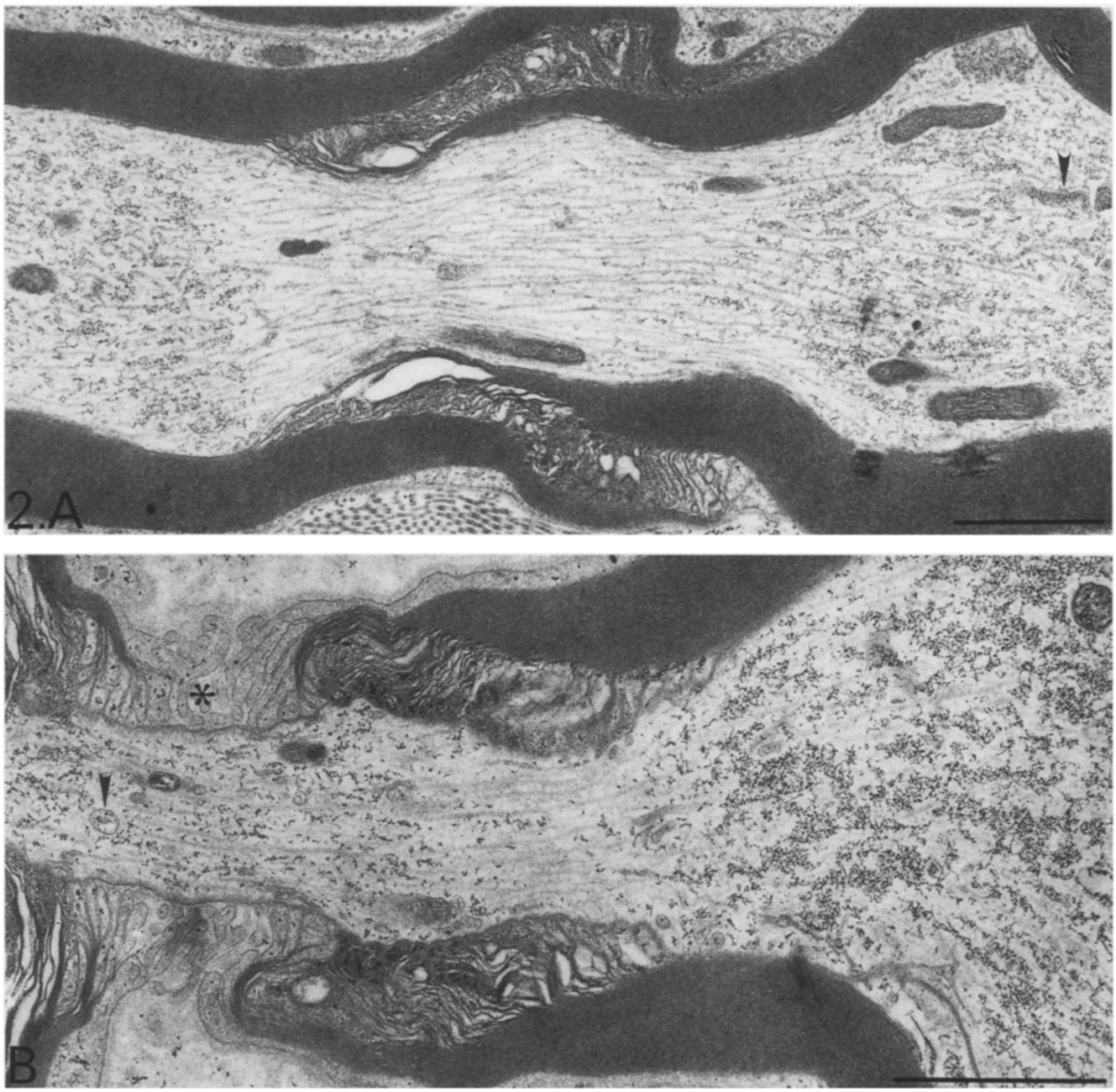

Fig. 2. A Ca^{++} precipitate in myelinated fibers. The amount of non-membrane bound axoplasmic precipitate consistently decreased in the region of the axoplasm beneath the Schmidt-Lanterman clefts. Calcium precipitate is seen also in endoplasmic reticulum (*arrowhead*) and mitochondria. ×26220, stained with uranyl acetate. *Bar*=1 μm. **B and C** Ca^{++} precipitate at the node of Ranvier in myelinated fibers. The amount of precipitate decreased consistently in the region of axoplasm under the paranodal loops of myelin. Precipitate is also seen in the Schwann cell cytoplasm near the node and in the Schwann cell microvilli (*asterisk*), as well as in vesicular profiles of endoplasmic reticulum (*arrowhead*) and mitochondria in the axon. **B** ×34200; **C** ×16650, stained with uranyl acetate. *Bar*=1 μm

creased (Fig. 2B, C). In a few instances, the density of precipitate did not change across the node. Ca^{++} precipitate was often seen in the Schwann cell microvilli at the node.

In the myelin, Ca^{++} precipitate occurred in the paranodal loops about the nodes of Ranvier (Fig. 3A) and within the Schmidt Lanterman clefts (Fig. 3B). In the Schwann cell perikaryon Ca^{++} was seen in the nucleus, mitochondria, smooth endoplasmic reticulum and Golgi (Fig. 4A) and was particularly dense in the cytoplasm near the nodes of Ranvier (Fig. 5A).

Endoneurium and perineurium

Scattered precipitate was seen in the endoneurial space outside axons particularly around the collagen fibril bundles (Fig. 4B). The perineurial cells contained prominent Ca^{++}

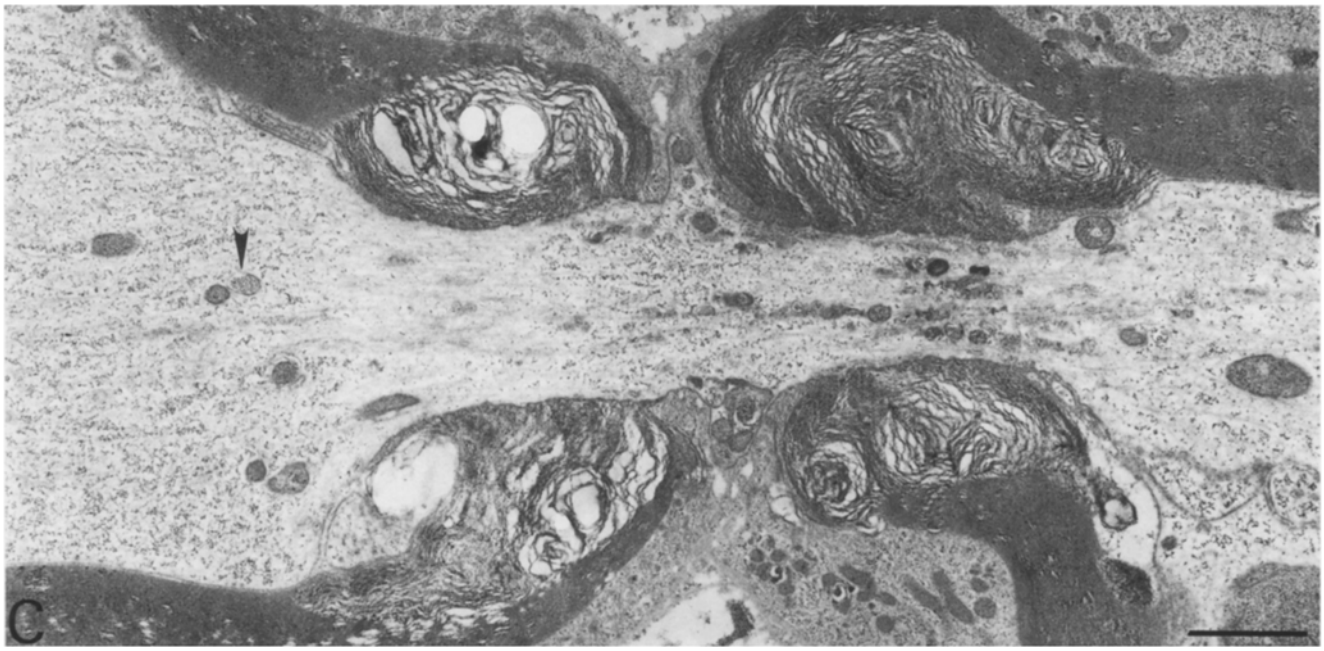

precipitate predominantly within pinocytotic vesicles and vesicular profiles of smooth endoplasmic reticulum (Fig. 4C).

Dorsal root ganglion

Ca^{++} precipitate was found diffusely within both dark and light DRG neurons (Fig. 5). Precipitate was particularly prominent in the euchromatin regions of the nucleus but spared the nucleoli and the nuclear bodies. In the cytoplasm Ca^{++} was seen free in the cytosol, as well as within the mitochondria, Golgi, large vesicles and mutivesicular bodies, but was always absent from the rough endoplasmic reticulum, ribosomal accumulations and lysosomes. Precipitate in satellite cells and vascular endothelial cells was seen principally in vesicular profiles and mitochondria.

Muscle and neuromuscular junction

In the neuromuscular junction, Ca^{++} was found most prominently in the synaptic vesicles. Virtually every synaptic vesicle contained precipitate (Fig. 6). Precipitate was also found in mitochondria and within smooth endoplasmic reticulum in the nerve terminal. Ca^{++} was found within the muscle in the postsynaptic infoldings, although both the primary and secondary clefts themselves were free of Ca^{++} (Fig. 6). Within the muscle, Ca^{++} was found between the myofibrils, particularly in mitochondria and sarcoplasmic reticulum and in the nucleus. Precipitate was rarely found within T-tubules (Fig. 6, insert).

Discussion

Using the oxalate-pyroantimonate technique, we have determined the ultrastructural localization of Ca^{++} within rat sciatic nerve. The question of the distribution of Ca^{++} in neurons has been addressed previously by other investigators, and the results reported depend on the method used. Oschman et al. (1974), using the addition of Ca^{++} during fixation to create precipitates at Ca^{++} binding sites demonstrated deposits along the squid axon plasma membrane, within mitochondria and along the Schwann cell plasma membrane. Similarly, Parducz and Joo (1976) using the same method demonstrated large precipitates within mitochondria in sympathetic ganglia in vivo.

The accumulation of exogenous Ca^{++} within the nerve cell has been studied using Ca^{++} loading in vitro prior to fixation. Hillman and Llinas (1974) showed that fixing the squid stellate ganglion in presence of 5–15 m*M* Ca^{++} after either injecting 500 m*M* Ca^{++} or immersing the ganglion in artificial seawater containing 50 m*M* Ca^{++}, created precipitates on the axolemma, in mitochondria and cisterns. And using oxalate to chelate calcium, Henkart et al. (1978) showed that squid giant axon accumulated Ca^{++} precipitates in smooth endoplasmic reticulum and mitochondria after stimulation in artificial seawater containing 112 m*M* calcium. Chan et al. (1984) studied Ca^{++} distribution in cat sciatic nerve exposed to various levels of Ca^{++} in vitro. They used a glutaraldehyde pyroantimonate fixative which apparently localizes a pool of predominantly membrane bound Ca^{++} and found precipitate in the membrane of the smooth endoplasmic reticulum and mitochondria as well as in the paranodal loops of the Schwann cells and in the ground substance surrounding the node of Ranvier. Each of these studies demonstrated the in vitro sequestration of exogenous Ca^{++} in organelles within neurons.

Duce and Keen (1978), using osmium pyroantimonate as a primary fixative without either Ca^{++} loading or Ca^{++} treatment during fixation, demonstrated deposits along smooth endoplasmic reticulum, in mitochondria and along the axolemma of rat dorsal root. All their precipitates appeared membrane bound, reflecting the presence of endogenous Ca^{++} on membrane binding sites. Borgers et al. (1977) developed a modification of the basic pyroantimonate technique in using oxalate to chelate Ca^{++} specifically during the primary fixation, while other cations are washed out. In contrast to other methods of Ca^{++} localization, their method produces precipitate which is not particularly

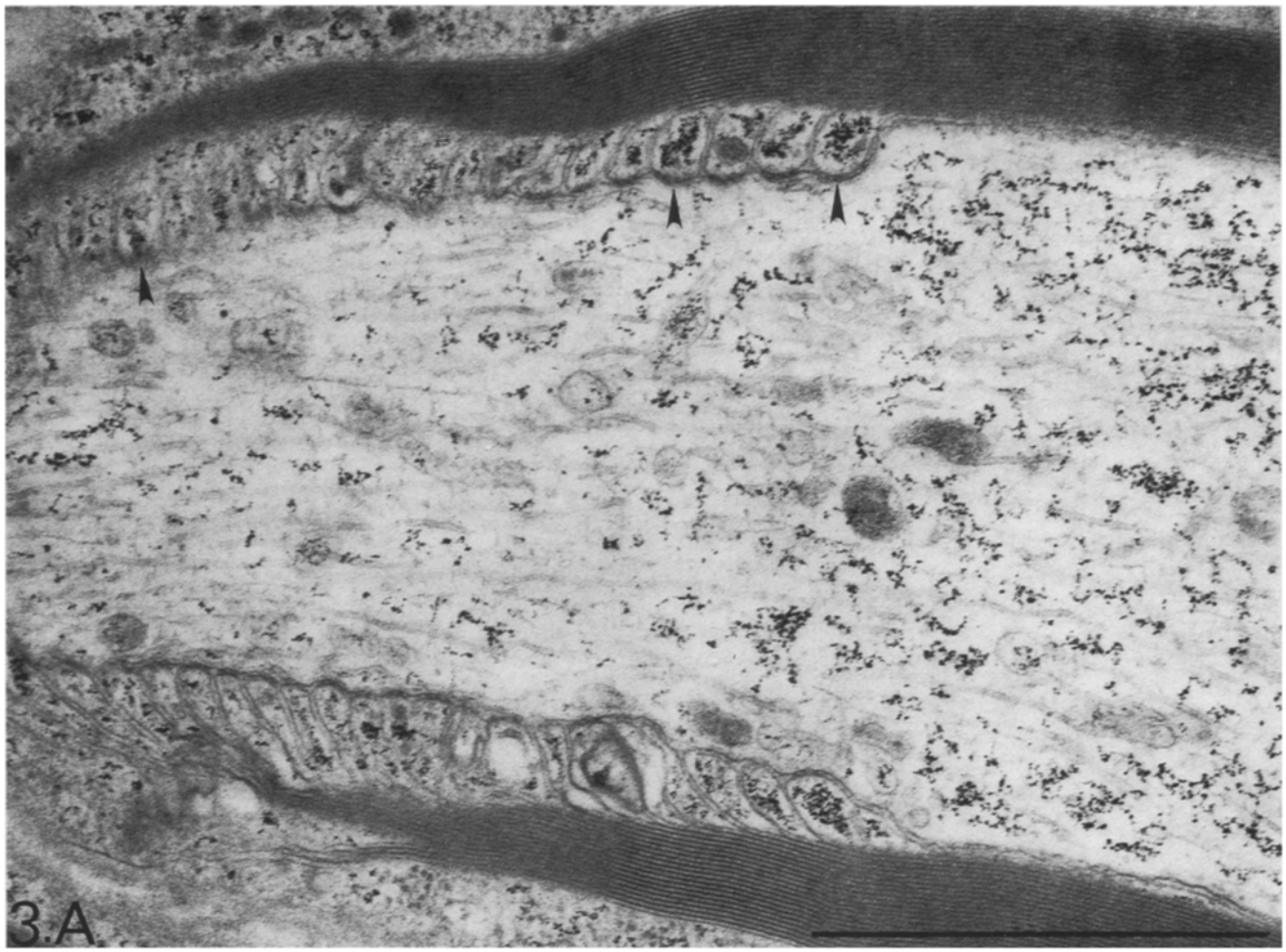
3.A


B

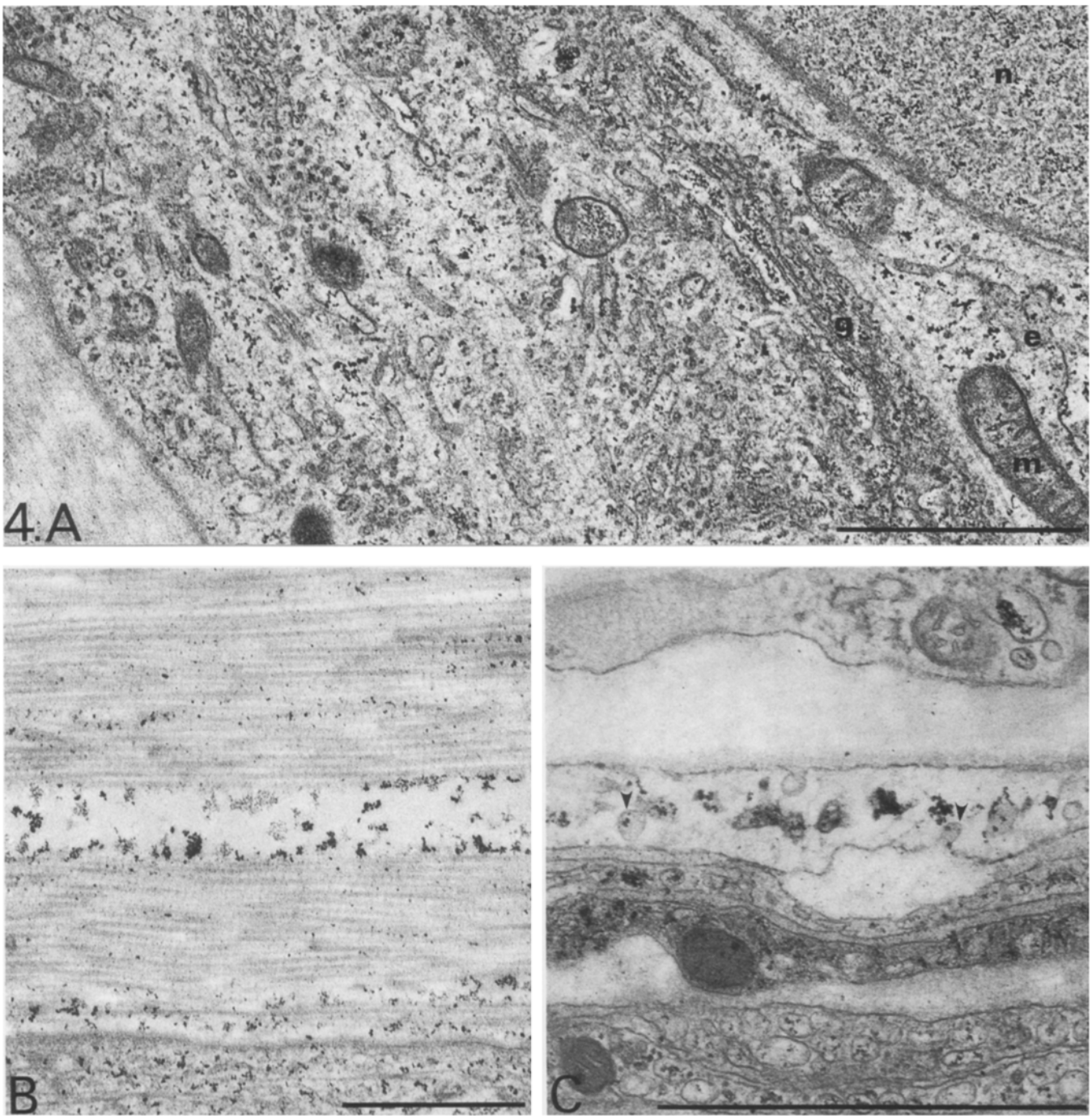

Fig. 4. **A** Ca^{++} precipitate in the Schwann cell perikaryon. Precipitate is seen in the nucleus (*n*), mitochondria (*m*), Golgi (*g*) and smooth endoplasmic reticulum (*e*). ×43800, stained with lead citrate. *Bar* = 1 μm. **B** Endoneurial Ca^{++} precipitate around collagen fibril bundles. ×32000, stained with uranyl acetate. *Bar* = 1 μm. **C** Ca^{++} precipitate in the perineurial cells. Precipitate is found predominantly in endoplasmic reticulum within the cells. Pinocytotic vesicles containing Ca^{++} precipitate are also seen (*arrowheads*). ×72000, stained with lead citrate. *Bar* = 1 μm

Fig. 3. **A** Ca^{++} precipitate within the paranodal loops of myelin about the node of Ranvier (*arrowheads*). Note the gradient of precipitate within the axoplasm in the same region. ×64500, stained with uranyl acetate. *Bar* = 1 μm. **B** Ca^{++} precipitate within the Schmidt-Lanterman cleft of myelinated fiber (*arrowheads*). ×53500, unstained. *Bar* = 1 μm

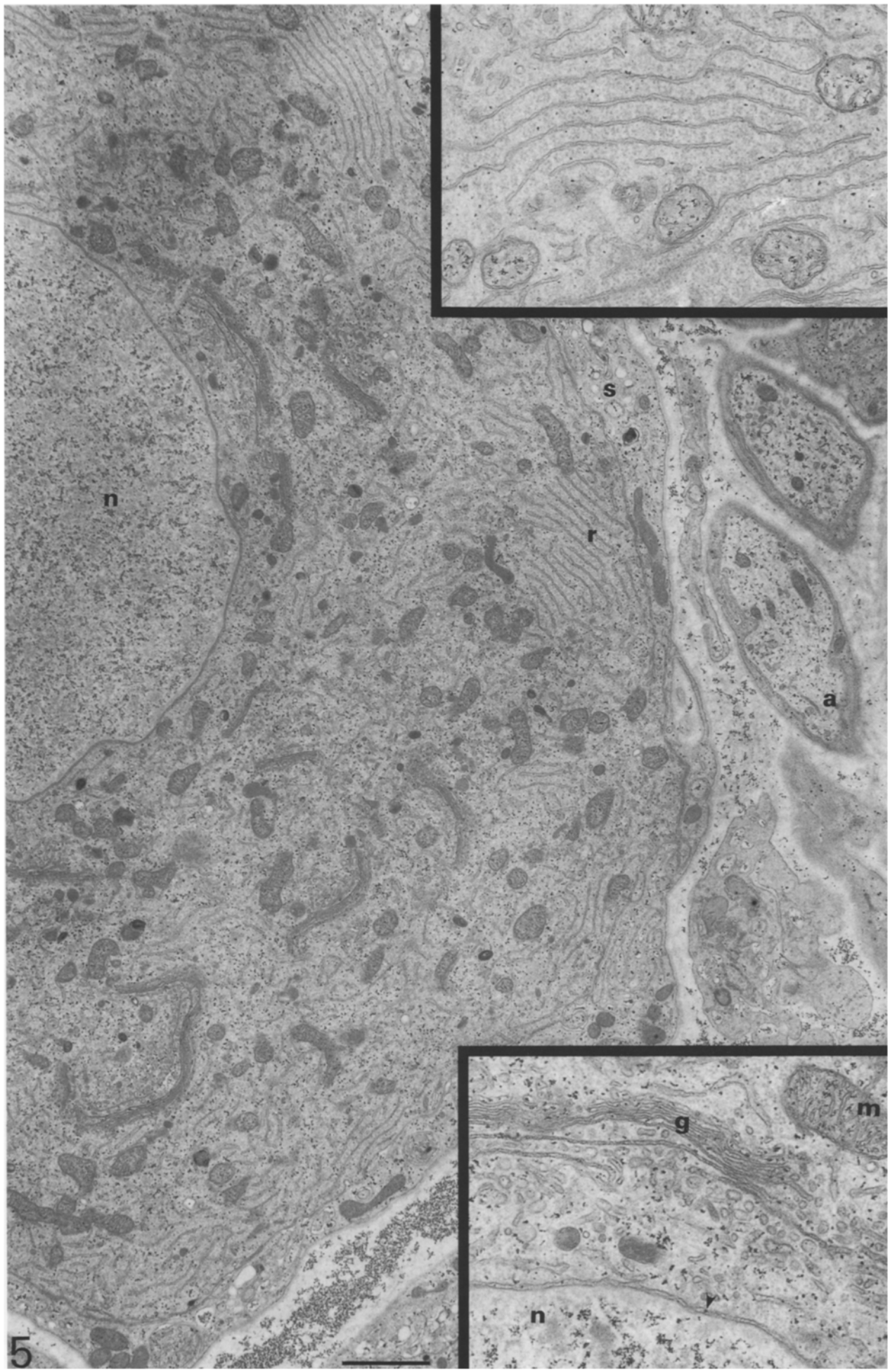

5

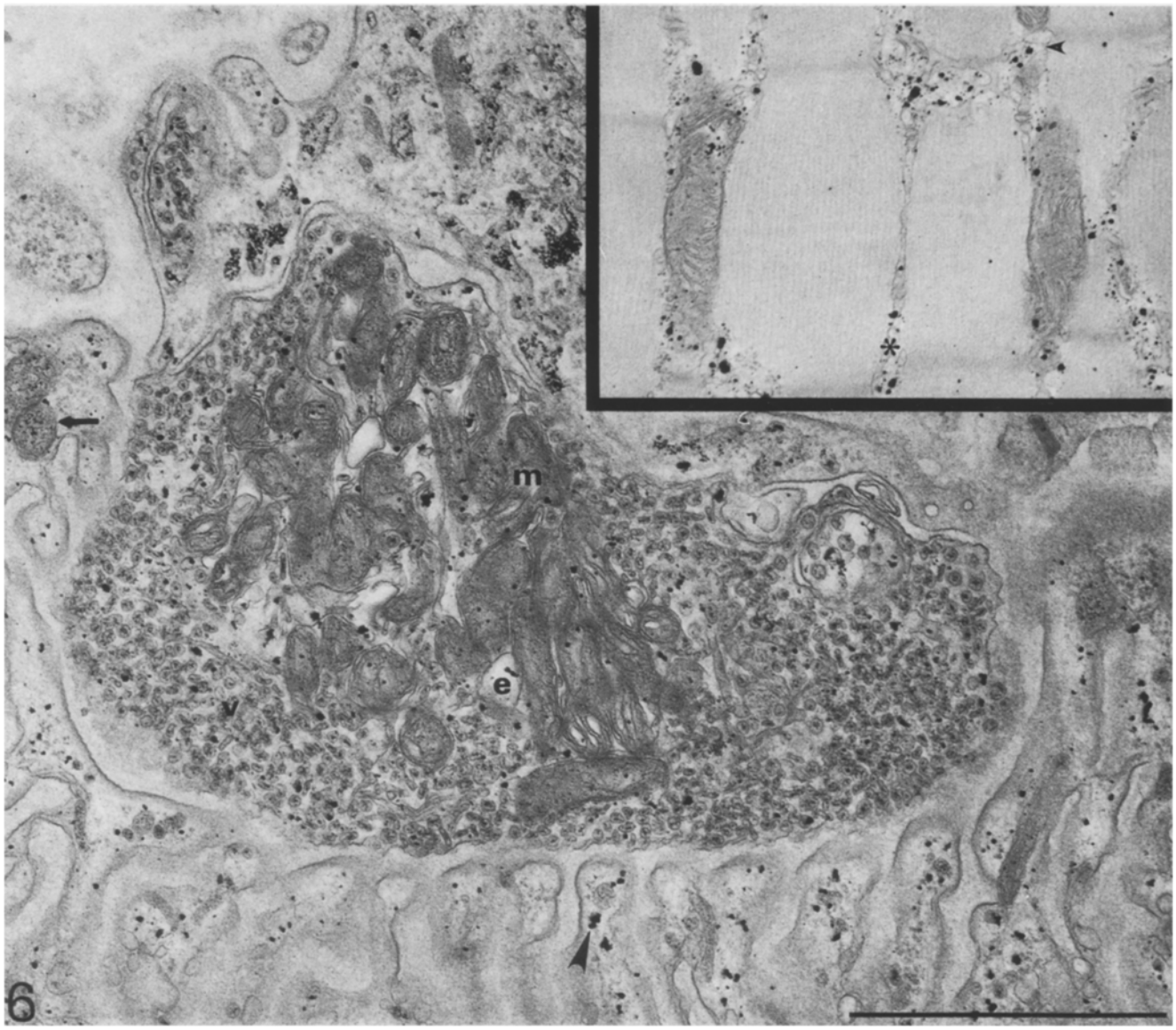

Fig. 6. Neuromuscular junction. Ca^{++} precipitate is seen in synaptic vesicles (*v*), mitochondria (*m*) and smooth endoplasmic reticulum (*e*) in the presynaptic terminal. In the muscle, calcium is seen beneath the postjunctional folds (*arrowheads*) and in postjunctional mitochondria (*arrow*). ×53100, stained with lead citrate. *Bar*=1 μm. *Insert.* Muscle. Ca^{++} precipitate is seen within the sarcoplasmic reticulum (*asterisk*), terminal vesicles (*arrow*) and mitochondria. ×37000, stained with lead citrate

associated with membranes. Borgers has proposed that this is because oxalate traps a mobile pool of calcium, in contrast to other methods which measure either Ca^{++} binding sites or a membrane bound pool of Ca^{++} perhaps bound to acidic phospholipids. Using this method, Ohara et al. (1979) and Wade et al. (1980) have studied the distribution of Ca^{++} in central nervous system neurons. We have used the Borgers et al. (1977) method with two modifications. We have added 90 m*M* oxalate to the buffers used to preperfuse in addition to the oxalate in the primary fixative, and we perfused with fixative for 1 h. Like the reports of Borgers et al. (1977) in cardiac muscle, we found a fine reticular precipitate throughout the axoplasm not particularly associated with membranes.

Using this variation of the method, we have found patterns of precipitate which are reproducible from experiment to experiment. X-ray microanalysis confirmed the presence of Ca^{++} within the precipitate, and treatment of the grids with EGTA removed the precipitate. In agreement with biochemical data which suggests that endoplasmic reticu-

Fig. 5. Dorsal root ganglion neuron. Ca^{++} precipitate is seen within the nucleus (*n*). In the cytoplasm, the precipitate appears to spare the domains of the rough endoplasmic reticulum (*r*). Ca^{++} is also seen in the satellite cells (*s*) and axons (*a*). ×17330, stained with uranyl acetate. *Bar*=1 μm. *Upper insert.* High power view of rough endoplasmic reticulum from the cell shown. The area is almost devoid of precipitate, except in mitochondria. ×32800, stained with uranyl acetate. *Lower insert.* High magnification view of the perinuclear region of the dorsal root ganglion cell. Ca^{++} is seen within the euchromatin region of the nucleus (*n*), in the Golgi (*g*) and in mitochondria (*m*). A small amount of precipitate is seen within the nuclear membrane (*arrowheads*). ×46560, stained with uranyl acetate

lum may act as both a source and a sink of intracellular Ca^{++} in non-muscle cells (Somlyo 1984), and that mitochondria contain 20%–30% of cell Ca^{++} (Bygrave 1978), we found precipitate within both these structures. Other ultrastructural methods have demonstrated the presence within mitochondria and smooth endoplasmic reticulum of available Ca^{++} binding sites (Oschman et al. 1974), endogenous membrane bound Ca^{++} (Duce and Keen 1978) and the sequestration of exogenously applied Ca^{++} (Henkart et al. 1978). The free precipitate within the mitochondria and smooth endoplasmic reticulum which we found presumably represents a mobilizable pool of Ca^{++} within these organelles and is similar to the distribution described by Probst (1986) in the carp tectum.

We also found Ca^{++} precipitate in synaptic vesicles of the neuromuscular junction. Similar precipitates have been described in synaptic vesicles of brain (Ohara et al. 1979; Probst 1986), retina (Van Reempts et al. 1982) and in the microvesicles of the neurohypophysis (Shaw and Morris 1980) and chromaffin granules of the adrenal medulla (Ravazolla 1976). Ca^{++} binding sites using the Oschman and Wall techniques have been demonstrated in frog neuromuscular junction (Pappas and Rose 1976). In adrenal chromaffin granules, a Ca^{++} concentration of 5–20 m*M* has been measured using biochemical techniques, and although both Ca^{45} uptake into granules and a sodium-Ca^{++} exchange in chromaffin granule membrane has been demonstrated, the role of Ca^{++} in these vesicles is not known (Winkler and Westhead 1980).

At the cell body, Ca^{++} precipitate appeared in the nucleus, in agreement with other reports and with the biochemical evidence that the nucleus contains a large fraction of the cell Ca^{++} (Maunder et al. 1977). The Golgi cisternae and vesicles contained Ca^{++} precipitate which accords with their role in the packaging of macromolecules into vesicles and endoplasmic reticulum both of which contain Ca^{++} in the axon and at the terminal region. The absence of Ca^{++} precipitate in rough endoplasmic reticulum agrees with biochemical data from other cell types (Immelman and Soling 1983).

A novel finding was the distribution of the fine reticular pattern of precipitate in specific domains within the cell, not related to the sequestration in organelles. Within the axoplasm, precipitate was linearly oriented, apparently along neurofilaments. A similar distribution of precipitate in frog and lizard axons was described by Krishnan and Singer (1974), though their study lacks X-ray microanalysis or EGTA controls to determine the identity of trapped cations. We found less precipitate along microtubules despite good preservation of microtubules in our preparation. High concentrations of Ca^{++} depolymerize microtubules in vitro (Schliwa 1976), so the relative exclusion of Ca^{++} from these areas may play a role in maintaining microtubular integrity.

In addition to the ultrastructural domains within the axon, there appeared also to be larger domains along the length of the axon where the amount of precipitate varied in a predictable fashion. We found that beneath the Schmidt-Lanterman clefts as well as in the paranodal region, the amount of precipitate decreased significantly, while the amount of precipitate between these regions was relatively constant in a given axon. The heterogeneity in distribution suggests that while average free Ca^{++} within the cell is 10^{-7} *M*, the actual concentration in regions outside organelles may vary considerably. There are several possible explanations for this finding. These gradients may represent heterogeneity in binding sites for Ca^{++} within the axoplasmic matrix. Alternatively, we favor the possibility that they reflect the distribution of regions of active Ca^{++} flux in the nerve. There is evidence to suggest that Ca^{++} enters the nerve both at the synaptic terminal and through the axolemma of unmyelinated axons (Baker and DiPolo 1984). Both biochemical and morphologic evidence suggests that the smooth endoplasmic reticulum is probably the major organelle which actively sequesters calcium, with the mitochondria serving as a larger back-up sink. But the axon in vivo is in a steady state in which influx and sequestration must be balanced over time by release and ultimately extrusion of calcium. The regions of low density of precipitates in the axoplasm under the Schmidt-Lanterman clefts and paranodally may be the regions where Ca^{++} is extruded across the axolemma, with the gradient of Ca^{++} serving to draw Ca^{++} into that area by diffusion followed by the active extrusion of calcium. The presence of Ca^{++} precipitate in the Schmidt-Lanterman clefts and dense deposits in the paranodal loops of Schwann cell cytoplasm would fit with this hypothesis. Landon and Hall (1976) have proposed that Schmidt-Lanterman clefts may function as a channel for the transport of materials across the myelin sheath.

The distribution of precipitate also suggests that Ca^{++} influx may occur preferentially at the node of Ranvier, with extrusion occurring across the axolemma in the paranodal regions. Chan et al. (1984) have shown that after incubation of sciatic nerve segments in Ca^{++} containing solutions, Ca^{++} appeared to accumulate within nodal axoplasm which is consistent with our results. This may represent the "leak" of Ca^{++} down its electrochemical gradient through sodium channels. These channels are restricted to the node of Ranvier in myelinated fibers (Ellisman and Levinson 1982) and in the squid giant axon, this leak accounts for 70% of the resting influx of Ca^{++} (DiPolo et al. 1982). The alternative possibility that Ca^{++} channels are localized to the nodal membrane will require pharmacologic and immunocytochemical investigation. The presence of Ca^{++} within Schwann cell microvilli, though, suggests that they may serve as a local reservoir of Ca^{++} in a manner similar to that which has been proposed for sodium (Landon and Hall 1976) and may regulate its availability to the nodal axolemma.

We have demonstrated that the precipitate whose distribution we describe is specifically Ca^{++} pyroantimonate. We cannot determine the threshold of sensitivity for the detection of Ca^{++} by this method, and as considered above, there are likely different pools of calcium which are selected by the different ultrastructural techniques. A vexing problem for which there is no absolute answer is whether the ultrastructural localization defined by electron microscopy represents the distribution in vivo of calcium. This question is faced in some form by most all histochemical, immunocytochemical and autoradiographic techniques, and the evidence that calcium is effectively retained and localized to its sequestration sites in the various ultrastructural methods has been reviewed recently by Probst (1986). More recently, Przelecka et al. (1986) have shown that the quantitative measurement of calcium in oocytes after ammonium oxalate fixation is similar to that measured after freeze drying (Przelecka et al. 1980). In the experiments reported here, the heterogeneous and reproducible distribution of the pre-

cipitate agrees with biochemical data of Ca^{++} sequestration. We have also found that following axonal injury, specific changes occur in some aspects of that distribution (Mata et al. 1986), which lends further support to the notion that the pattern which we describe is biologically significant.

Acknowledgements. This work was supported by VA Merit Review Grants to Dr. Mata and to Dr. Fink.

The authors would like to express appreciation to Dr. W.C. Bigelow and Ms. H. Honke from the Department of Materials and Metallurgical Engineering at the University of Michigan for their assistance in the microanalysis of the spectra.

Preliminary results of this study were presented in abstract form at the meetings of the American Academy of Neurology in April, 1985 and at the Society for Neuroscience in October, 1985.

References

Baker PF, DiPolo R (1984) Axonal calcium and magnesium homeostasis. In: Baker PF (ed) Current topics in membranes and transport, vol 22. Academic Press, New York, pp 195–247

Blaustein MP, Ratzlaff RV, Kendrick NC, Schweitzer ES (1978) Calcium buffering in presynaptic nerve terminals. Evidence for involvement of a nonmitochondrial ATP-dependent sequestration mechanism. J Gen Physiol 72:15–41

Borgers M, deBrabander M, Van Reempts J, Awouters F, Jacob WA (1977) Intranuclear microtubules in lung mast cells of guinea pig in anaphylactic shock. Lab Invest 37:1–7

Bygrave FL (1978) Mitochondria and the control of intracellular calcium. Biol Rev 53:43–78

Campbell AK (1983) Intracellular calcium: its universal role as regulator. John Wiley, New York

Carafoli E, Crompton M (1976) Calcium ions and mitochondria. In: Duncan CJ (ed) Calcium in biological systems. Cambridge University Press, Cambridge, pp 89–115

Chan SY, Ochs S, Jersild RA (1984) Localization of calcium in nerve fibers. J Neurobiol 15:89–108

DiPolo R, Rojas H, Beauge L (1982) Ca entry at rest and during prolonged depolarization in dialyzed squid axons. Cell Calcium 3:19–41

Duce IR, Keen P (1978) Can neuronal smooth endoplasmic reticulum function as a calcium reservoir? Neuroscience 3:837–848

Ebashi S, Endo M (1968) Calcium and muscle contraction. Prog Biophys Mol Biol 18:125–183

Ellisman MH, Levinson R (1982) Immunocytochemical localization of sodium channel distributions in the excitable membranes of electrophorus electricus. Proc Natl Acad Sci USA 79:6707–6711

Endo M (1977) Calcium release from the sarcoplasmic reticulum. Physiol Rev 57:71–108

Henkart MP, Reese TS, Brinley FJ (1978) Endoplasmic reticulum sequesters calcium in the squid giant axon. Science 202:1300–1302

Hillman DE, Llinas R (1974) Calcium-containing electron-dense structures in the axons of the squid giant synapse. J Cell Biol 61:146–155

Immelman A, Soling HD (1983) ATP dependent calcium sequestration and calcium/ATP stoichiometry in isolated microsomes from guinea pig parotid glands. FEBS Lett 162:406–410

Krishnan N, Singer M (1974) Localization of cations in the peripheral nerve fiber by the K-pyroantimonate method. Exp Neurol 42:191–205

Landon DN, Hall S (1976) The myelinated nerve fibre. In: Landon DN (ed) The peripheral nerve. Chapman and Hall, London, pp 1–105

Mata M, Staple J, Fink DJ (1986) Changes in intra-axonal calcium distribution following nerve crush. J Neurobiol 17:449–467

Maunder CA, Yarom R, Dubowitz V (1977) Electron microscopic X-ray microanalysis of human and diseased human muscle. J Neurol Sci 33:323–334

Ochs S, Worth R, Chan SY (1977) Calcium requirement for axoplasmic transport in mammalian nerve. Nature 270:748–750

Ohara PT, Wade CR, Lieberman AR (1979) Calcium storage sites in axon terminals and other components of intact C.N.S. tissue: studies with a modified pyroantimonate technique. J Anat 129:869

Oschman JL, Hall TA, Peter PD, Wall BJ (1974) Association of calcium with membranes of squid giant axon. J Cell Biol 61:156–163

Pappas GD, Rose S (1976) Localization of calcium deposits in the frog neuromuscular junction at rest and following stimulation. Brain Res 103:362–365

Parducz A, Joo R (1976) Visualization of stimulated nerve endings by preferential calcium accumulation of mitochondria. J Cell Biol 69:513–517

Probst W (1986) Ultrastructural localization of calcium in the CNS of vertebrates. Histochemistry 85:231–239

Przelecka A, Sobota A, Burovina IV, et al. (1980) Calcium content and distribution in egg vesicles of Galleria mellonella (lepidoptera) as determined by X-ray microanalysis. Histochemistry 67:321–329

Przelecka A, Allakhverdov BL, Glowacka SK et al. (1986) Ultracytochemical localization and microprobe quantitation of calcium stores in the insect oocyte. Histochemistry 85:163–168

Ravazolla M (1976) Intracellular localization of calcium in the chromaffin cells of the rat adrenal medulla. Endocrinology 98:950–953

Roomans GM (1980) Quantitative X-ray microanalysis in thin sections. In: Hayat MA (ed) X-ray microanalysis in biology. University Park Press, Baltimore, pp 401–453

Rubin RP (1970) The role of calcium in the release of neurotransmitter substances and hormones. Pharmacol Rev 22:389–423

Schamber FW, Wodke NF, McCarthy JJ (1977) Least squares fit with digital filter: the method and its application to EDS spectra. In: Beamon DR, Ogilvie RE, Wittry DB (eds) Eighth International Conference in X-Ray Optics Microanalysis. Pendell, Midland, MI, p 98A

Schlaepfer WW, Lee C, Lee V, Zimmerman VJP (1985) An immunoblot study of neurofilament degradation in situ and during calcium-activated proteolysis. J Neurochem 44:502–509

Schliwa M (1976) The role of divalent cations in the regulation of microtubule assembly. J Cell Biol 70:527–540

Shaw FD, Morris JF (1980) Calcium localization in the rat neurohypophysis. Nature 287:56–58

Somlyo AP (1984) Cellular site of calcium regulation. Nature 309:316–317

Theron JJ, Meyer BJ, Boekkoi S, Loots JM (1975) Ultrastructural localization of calcium in peripheral nerve of the rat. S Afr Med J 459:1795–1798

Van Reempts J, Borgers M, Offner F (1982) Ultrastructural localization of calcium in the rat retina with a combined oxalate-pyroantimonate technique. Histochem J 14:517–522

Wade CR, Ohara PT, Lieberman AR (1980) Calcium localization in normal and degenerating myelinated nerve fibres of the CNS. J Anat 130:641–644

Wick SM, Hepler PK (1982) Selective localization of intracellular Ca^{++} with potassium antimonate. J Histochem Cytochem 31:1190–1204

Williams R, Walker W (1967) Cation balance in biological systems. J Am Med Assoc 210:18–22

Winkler H, Westhead E (1980) The molecular organization of adrenal chromaffin granules. Neuroscience 5:1803–1823